Large-Angle Pion-Proton Elastic Scattering at High Energies*

J. Orear, R. Rubinstein,† D. B. Scarl,‡ and D. H. White
Laboratory of Nuclear Studies, Cornell University, Ithaca, New York
and
A. D. Krisch
The University of Michigan, Ann Arbor, Michigan
and
Laboratory of Nuclear Studies, Cornell University, Ithaca, New York
and
W. R. Frisken,# A. L. Read,§ and H. Ruderman‖
Brookhaven National Laboratory, Upton, New York

(Received 18 July 1966)

Differential cross sections for elastic $\pi^{\pm}$-p scattering have been measured at lab momenta of 8 and 12 GeV/c in a momentum-transfer region corresponding to $1.2 \leq -t \leq 6$ (GeV/c)^2. Also, differential cross sections near 180° were measured for 4 and 8 GeV/c pions. At momentum transfers greater than $-t=2$ (GeV/c)^2, the π-p cross sections drop much faster with increasing angle than the corresponding p-p cross sections. Also, in the region $-t \simeq 1.3$ (GeV/c)^2, there is structure in the π-p angular distribution but not in the p-p angular distribution. At $-t \simeq 3$ (GeV/c)^2, the drop in cross section appears to stop and from then on the angular distribution is consistent with isotropy. But in the angular region 170° to 180°, the cross sections have become much larger, and sharp backward peaks are observed. Information is given on the energy and charge dependences and widths of these backward peaks.

1. INTRODUCTION

THE purpose of this experiment was to obtain large-angle elastic-scattering angular distributions of pions on protons at high energies. Prior to this experiment, the highest energy large-angle results for pion-proton elastic scattering were from a 4-GeV/c π^+ liquid hydrogen bubble chamber experiment.[1] On the other hand, complete angular distributions for proton-proton elastic scattering were available up to 30 GeV.[2] One might expect some difference in p-p and π-p large-angle scattering due to the baryon "core" which is present in one case, but not the other. Prior to this experiment, pion-proton scattering results above 4 GeV were essentially in the diffraction peak region,[3,4] and these indicated similar angular distributions for the π-p and p-p systems. However, the results of the present experiment reveal differences in the π-p and p-p angular distributions at lab momenta of 8 and 12 GeV/c at angles larger than those studied in the previous experiments. At momentum transfers higher than $-t=2$ (GeV/c)^2, we find that the π-p cross sections drop much faster with increasing angle than the p-p. Also in the region $-t \simeq 1.3$ (GeV/c)^2 there is structure in the π-p angular distribution which does not appear in the p-p angular distribution.[5] At $-t \sim 3$ (GeV/c)^2 the drop in cross section appears to stop, and at higher momentum transfers the angular distribution is consistent with being isotropic.

A new phenomenon which was indicated in the π^+-p bubble chamber results[1] is the presence of a backward peak in the angular distribution. The preliminary results of this experiment at 4 and 8 GeV/c,[6] along with those of more recent experiments,[7–12] reveal rather sharp

* Research supported in part by the National Science Foundation and the U. S. Atomic Energy Commission. This research was performed using the Alternate Gradient Synchrotron at the Brookhaven National Laboratory.

† Present address: Brookhaven National Laboratory, Upton, New York.

‡ Present address: Physics Department, Polytechnic Institute of Brooklyn, Farmingdale, New York.

§ Present address: Laboratory of Nuclear Studies, Cornell University, Ithaca, New York.

‖ Present address: Physics Department, University of California, San Diego, La Jolla, California.

Present address: Physics Department, Case Institute of Technology, Cleveland, Ohio.

[1] Aachen-Berlin-Birminghan-Bonn-Hamburg-London-München Collaboration, Phys. Letters **10**, 248 (1964).

[2] G. Cocconi, V. T. Cocconi, A. D. Krisch, J. Orear, R. Rubinstein, D. B. Scarl, B. T. Ulrich, W. F. Baker, E. W. Jenkins, and A. L. Read, Phys. Rev. **138**, B165 (1965).

[3] K. J. Foley, S. J. Lindenbaum, W. A. Love, S. Ozaki, J. J. Russell, and L. C. L. Yuan, Phys. Rev. Letters **11**, 425 (1963).

[4] D. Harting, P. Blackall, B. Elsner, A. C. Helmholz, W. C. Middelkoop, B. Powell, B. Zacharov, P. Zanella, P. Dalpaiz, M. N. Cocacci, S. Focardi, G. Giacomelli, L. Monari, J. A. Beany, R. A. Donald, P. Mason, L. W. Jones, and D. O. Caldwell, Nuovo Cimento **38**, 60 (1965).

[5] A. R. Clyde, B. Cork, D. Keefe, L. T. Kerth, W. M. Layson, and W. A. Wenzel, University of California Radiation Laboratory Report No. UCRL-11441 (unpublished); A. R. Clyde, University of California Radiation Laboratory Report No. UCRL-16275 (unpublished).

[6] W. R. Frisken, A. L. Read, H. Ruderman, A. D. Krisch, J. Orear, R. Rubinstein, D. B. Scarl, and D. H. White, Phys. Rev. Letters, **15**, 309; **15**, 313 (1965).

[7] H. Brody, R. Lanza, R. Marshall, J. Niederer, W. Selove, M. Shocket, and R. Van Bert, Phys. Rev. Letters **16**, 828 (1966); **16**, 968 (1966).

[8] A. I. Alikhanov, G. L. Bayatyan, E. V. Brakhman, G. P. Eliseev, Yu. V. Galaktionov, L. G. Landsberg, V. A. Lyubimov, I. V. Sidorov, F. A. Yetch, and O. Ya. Zeldovich, Phys. Letters **19**, 345 (1965).

[9] A. S. Vovenko, B. N. Gus'kov, M. F. Likhachev, A. L. Lyubimov, Yu. A. Matulenko, I. A. Savin, and V. S. Stavinskii, JETP Pis'ma v Redaktsiyu **2**, 409 (1965) [English transl.: JETP Letters **2**, 255 (1965)].

[10] C. T. Coffin, N. Dikmen, L. Ettlinger, D. Meyer, A. Saulys, K. Terwilliger, and D. Williams, Phys. Rev. Letters **15**, 838 (1965).

[11] W. F. Baker, P. J. Carlson, V. Chabaud, A. Lundby, E. Michaelis, J. Banaigs, J. Berger, C. Bonnel, J. Duflo, L. Goldzahl, and F. Plouin, in Proceedings of the Oxford International Conference on High Energy Physics, 1965 (unpublished); (private communications).

[12] S. W. Kormanyos, A. D. Krisch, J. R. O'Fallon, K. Ruddick, and L. G. Ratner, Phys. Rev. Letters **16**, 709 (1966).

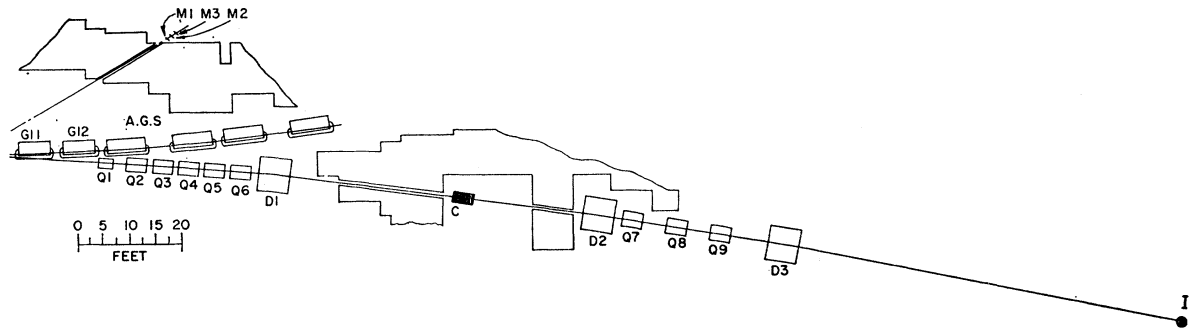

FIG. 1. Secondary beam at 4.5° from G10 target at Brookhaven AGS. Pions of desired momentum are focused at point I.

and striking backward peaks in both π^+-p and π^--p elastic scattering. The data presented in this paper were reported earlier in a preliminary form.[6] This paper presents a more refined analysis of the data and a more thorough discussion of the experimental details and theoretical implications. The results in their final form as presented here bear some quantitative, but not qualitative, differences from their preliminary form as presented in Ref. 6.

2. EXPERIMENTAL METHOD

A secondary beam[13] of positive or negative pions of 4–12 GeV/c was obtained from the Brookhaven AGS and scattered by a liquid hydrogen target. Counter telescopes were positioned to record momentum-analyzed scattered pions and recoil protons in coincidence.

A. Beam

The 27–30 GeV circulating proton beam of the Brookhaven AGS struck a 0.030-in.-diam beryllium wire target, one-half in. in length along the secondary beam direction placed at the upstream end of the G10 straight section. Secondaries which were produced at an angle of about 4.5° and within a solid angle of 0.2 msr were accepted by the quadrupole system Q_1-Q_6 (see Fig. 1) which formed a triplet lens, and focused an image of the beryllium target at collimator C. Quadrupoles Q_1, Q_2 focused horizontally, Q_3, Q_4 vertically, and Q_5, Q_6 horizontally. Each element of the lens consisted of two quadrupoles since a single magnet was unable to give the required focal length at the higher beam momenta.

Deflecting magnet D_1 bent the trajectories of particles of the desired momentum through an angle of 2.9° and sent them through the 40-in.-long collimator C. The collimator aperture was $\frac{1}{2}\times\frac{1}{2}$ in. for the 4- and 8-GeV/c beams giving a momentum resolution of $\pm 1\%$. At 12 GeV/c, the collimator was opened to 1×1 in. to increase the particle flux with a resulting momentum resolution of $\pm 2\%$.

Quadrupoles Q_7, Q_8, and Q_9 formed a second triplet lens which imaged the collimator aperture on the hydrogen target at I. Deflecting magnet D_2 bent the trajectories through an angle of 2.0° in order to recombine momenta. The final switching magnet D_3 bent the trajectories through an angle of 0.7° and was used to deflect the beam to a different area when it was shared with another experimental group. Further details concerning the beam design are available.[13]

The measured beam shape at the hydrogen target was ~0.8 in. wide by 1.0 in. high and is shown in Fig. 2. The upper limit on the vertical angular divergence as defined by the ratio of the D_3 aperture to the target distance was ± 2.5 mrad. The horizontal angular divergence as defined by the ratio of the Q_9 aperture to the target distance was ± 3 mrad. According to orbit calculations the actual angular divergences should be somewhat less than these upper limits.

For part of the run the beam was defined by scintillation counters B_1 and B_2 (see Figs. 3–5) which were 230 in. and 24 in. upstream from the hydrogen target, respectively. Counter B_1 was 3 in. diam by $\frac{1}{8}$ in. thick and B_2 was 1 in. wide by 1.5 in. high by $\frac{1}{8}$ in. thick. A 10-ft-

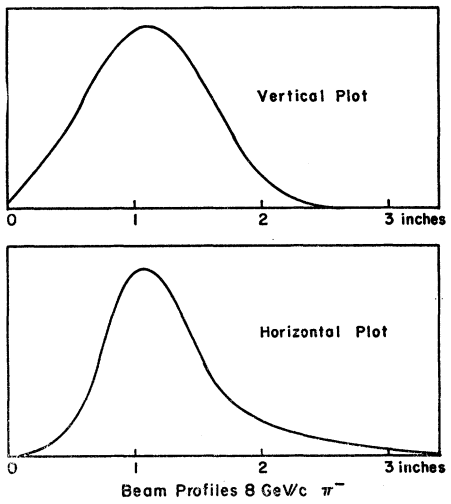

FIG. 2. Horizontal and vertical beam profiles for 8-GeV/c negative pions at position of hydrogen target taken with $\frac{1}{2}$-in.$\times\frac{1}{2}$-in. scintillation counter whose resolution has not been unfolded.

[13] A. L. Read and R. Rubinstein, Brookhaven National Laboratory Report No. 9213 (unpublished).

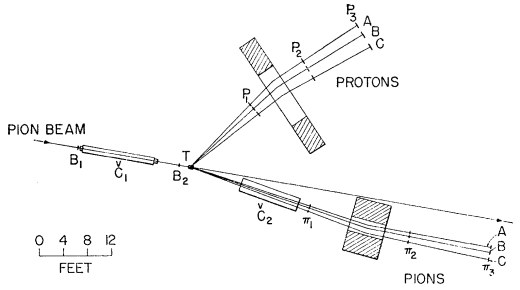

FIG. 3. Layout for Geometry 1. Several different magnet positions were used to obtain different regions of scattering angle.

long threshold gas Čerenkov counter,[14] C_1, using CO_2 gas as a radiator, counted pions, muons, and electrons.

In order to measure the number of muons in the beam, a short run was taken at each beam momentum with a 20-in.-diam scintillation counter placed behind 6 or 10 ft of iron 20 ft downstream of the hydrogen target. The percentage of electrons in the beam was determined from pressure curves of the gas Čerenkov counter.

Counters M_1, M_2, and M_3 in Fig. 1 provided a monitor of the AGS intensity.[2] The number of beam pions per 10^{11} AGS protons on the beryllium target was 2×10^5 at 4 and 8 GeV/c and 0.6×10^5 at 12 GeV/c. An average AGS pulse contained about 7×10^{11} protons producing a flux of about 10^6 pions on the hydrogen target at 8 GeV/c. The beam spill duration was about 250 msec every 2.4 sec. Under these conditions elastic scattering rates in the experiment varied from 20 per hour to one per 5 h.

B. Experimental Arrangement

Three different geometries were used for different regions of momentum transfer. In each geometry triple coincidences were taken between counter telescopes set at appropriate angles from the hydrogen target, one of which detected an entering beam pion, the second detected the scattered pion, and the third detected the recoil proton. In addition, the momenta of both the scattered and recoil particles were determined by the use of deflection magnets.

Geometry 1 (See Fig. 3)

This geometry was used at 8 and 12 GeV/c for scattering at momentum transfers in the region $1.2<-t<3.5$ (GeV/c)^2. In addition it was also used to measure proton-proton elastic scattering in this range for comparison.

The scattered pions were momentum analyzed by a standard AGS 30D72 deflection magnet with a gap 30 in. wide, 6 in. high, and 72 in. long, with an average field of 18 kG. The angles of bend ranged from 4° to 9° and the momentum resolution provided by the counter telescopes ranged from ±8 to ±17%. The recoil protons were momentum analyzed by a large-aperture magnet with a gap 120 in. wide, 24 in. high, and 36 in. long with an integrated field of 550 kG-in. The recoil proton trajectories were bent by 6° to 13°, providing a momentum resolution of between ±21 and ±45%. The scattered pion and recoil proton were detected in scintillation counter telescopes consisting of three counters each; in this geometry there were three such sets of counters, used to measure the elastic scattering at three different momentum transfers simultaneously.

For positive pions, the incident beam contained in the worst case (12 GeV/c) over three times as many protons as pions. Since the π^+-p and p-p elastic kinematics are almost identical for a given angle in the range under study, the only discrimination against p-p elastic scattering would be due to the beam Čerenkov counter C_1, which counted only pions and not protons. A major source of error could be a proton-proton elastic scattering falling into accidental coincidence with a beam pion. A large gas threshold Čerenkov counter C_2 in the scattered pion telescopes and sensitive only to pions was used to eliminate this possibility. Because the proton-proton elastic scattering cross sections were as much as 30 times larger than the pion-proton cross sections at the same momentum transfer, this Čerenkov counter was essential to the experiment.

The pion telescope Čerenkov counter was placed between the hydrogen target and the first set of scintillation counters, and was common to the three counter telescopes. Čerenkov light produced in SF_6 gas at atmospheric pressure was deflected by a thin aluminized Mylar mirror and focused by a 22-in. plastic Fresnel lens onto the 5-in. cathode of an Amperex 58 AVP photomultiplier. The efficiency of the counter could be measured using elastic scattering events with the negative pion beam, and was between 50 and 70% for the three channels at 8 GeV/c and between 90 and 100% at 12 GeV/c. The errors of these efficiency determinations ranged from ±0.02 to ±0.15.

Geometry 2 (See Fig. 4)

This arrangement was used only for incident π^- at 8 GeV/c, for momentum transfers between $-t=1.5$ and

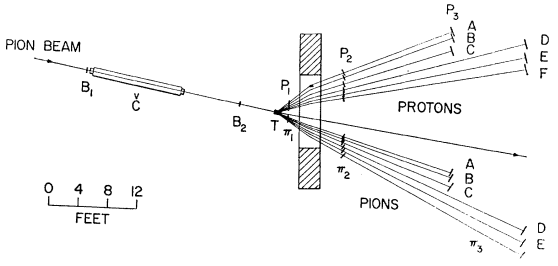

FIG. 4. Layout for Geometry 2 which was used for scattering angles up to 81° in the center-of-mass system.

[14] R. Rubinstein, Brookhaven National Laboratory Report No. 9466 (unpublished).

6.0 (GeV/c)^2. Both scattered pion and recoil proton were momentum analyzed by the large-aperture magnet. Larger solid angles (up to 12 msr in the center of mass) than in Geometry 1 could be used, and also a wider range of momentum transfer was covered. The integrated field of the magnet was 540 kG in., giving momentum resolutions of about $\pm 13\%$ for the pion and $\pm 16\%$ for the proton.

The results obtained with this geometry agreed well with those of Geometry 1 for the cases where scattering at the same momentum transfer was measured.

Geometry 3 (See Fig. 5)

For scattering of $\pi^{\pm}$ at 4 and 8 GeV/c near 180° in the center-of-mass system, an arrangement basically similar to Geometry 1 was used. The backward-scattered pion was analyzed in the large-aperture magnet, and the forward recoil proton in the 30D72 magnet. Scatterings at several different angles were measured simultaneously. Center-of-mass solid angles ranged from 0.5 to 1.5 msr, and the momentum resolution was between ± 6 to $\pm 12\%$. The center-of-mass angular acceptance of a typical counter channel was $\pm 1°$.

C. Counters

The scattered and recoil particles were detected in scintillation counter telescopes which consisted of two or three 0.5-in.-thick counters, ranging in size from 3×3 in. to 19×21 in. Larger areas were obtained by adding the signals of 2 or 4 adjacent counters. The scintillation material was Pilot type B, coupled by means of ultraviolet transmitting Plexiglas light pipes to RCA 7746 photomultipliers.

In most cases the last counter in each pion telescope determined the solid angle for the elastic scattering; the areas of the remaining pion and proton counters were increased from the kinematically determined areas by an amount calculated to allow for angular divergence in the incident beam, momentum spread of incident beam, beam spot size, target length, magnetic field uncertainties, and multiple scattering of the pion and proton. This additional area around the kinematically matched area of the proton counters was generally of the same area as the matched area.

D. Electronics

The individual counter signals were brought into an electronics trailer on 125 ft of RG8/U and 20 ft of RG58/U cable, and were standardized by Chronetics discriminators whose output pulse lengths determined the resolving times (~10 nsec) of the coincidence circuits. Coincident signals from the two scintillation counters and Čerenkov counter in the beam produced a "beam" pulse which was fanned out to each of the 2 to 6 scattered pion channels. In each channel the beam pulse

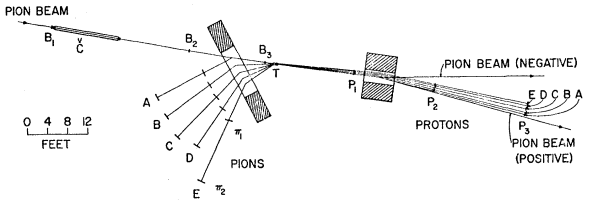

FIG. 5. Layout for Geometry 3 which was used for scattering angles near 180°.

and a coincidence signal from the 2 or 3 pion counters were put into a further coincidence to form a "beam + pion" pulse. Signals from the proton counters were put into coincidence to form a "proton" pulse. Finally the "beam + pion" pulse from each channel and the corresponding proton pulse were put into a 10-nsec coincidence to signify an elastic scattering event. Coincidences were also recorded between "beam + pion" pulses and pulses from kinematically unrelated proton telescopes to help in estimating the inelastic background. T.S.I. 10-Mc/sec scalers were used to record all coincidences, except those for the incident-beam particles where T.S.I. 100-Mc/sec prescalers were used.

The discriminator outputs of the last counter of both the pion and proton telescopes were sent to a time-to-height converter. A "beam + pion" and "proton" coincidence requirement with 50-nsec resolving time was used to gate these discriminator signals. The output pulse-height spectrum from the time-to-height converter corresponded to the difference of arrival times of scattered pions and protons at the last counters in their telescopes. For a block diagram and more details of this technique, see Ref. 2.

Eight time-to-height converting circuits were available simultaneously to verify the time correlation in the pion and proton telescopes. Rather than using eight pulse-height analyzers, 1 two-dimensional 1600 channel R.I.D.L. pulse-height analyzer was used to store the eight inputs in eight separate regions of its memory. A 16-channel routing circuit made use of one of the two analog-to-digital converters to organize the memory into 16 parallel 100-channel analyzers. These time correlated data were taken in the elastic coincidence channels and in some "crossed" channels simultaneously. The time spectra showed a peak of width about 2 nsec due to elastic scattering events, and in some cases a uniform background due to accidental coincidences. In most cases the number of accidental coincidences was so small as to be undetectable, but in some of the backward-scattering measurements, with high individual telescope counting rates, the accidentals made up 75% of the total counting rate. In all cases the counting rate recorded on the scalers and that recorded on the pulse-height analyzer agreed well, so the analyzer data provided assurance of the correct operation of the detection system and in those few experiments that had large accidental background subtraction allowed an acci-

TABLE I. Elastic scattering cross sections obtained using Geometries 1 and 2.

Incident particle	P_0 (GeV/c)	$\cos\theta_{c.m.}$	$-t$ (GeV/c)^2	$(d\sigma/d\omega)_{c.m.}$ (μb/sr)	$d\sigma/dt$ (μb/(GeV/c)^2)
π^-	8	0.8305	1.20	34.3 ±3.4	30.4 ±3.1
		0.7881	1.50	17.0 ±2.0	15.1 ±1.8
		0.7542	1.74	7.38 ±0.66	6.55 ±0.58
		0.7175	2.00	3.05 ±0.73	2.71 ±0.65
		0.6822	2.25	0.64 ±0.09	0.57 ±0.08
		0.6469	2.50	0.23 ±0.07	0.20 ±0.06
		0.6158	2.72	0.053±0.021	0.047±0.019
		0.5763	3.00	0.073±0.022	0.064±0.019
		0.5057	3.50	0.118±0.035	0.104±0.031
		0.4350	4.00	0.063±0.042	0.056±0.038
		0.2938	5.00	0.094±0.046	0.083±0.041
		0.1526	6.00	<0.07	<0.06
π^+	8	0.8305	1.20	37.8 ±3.4	33.5 ±3.0
		0.7881	1.50	16.7 ±1.7	14.8 ±1.5
		0.7542	1.74	8.10 ±0.89	7.18 ±0.79
		0.7175	2.00	3.75 ±0.64	3.33 ±0.57
		0.6822	2.25	1.00 ±0.21	0.89 ±0.19
		0.6469	2.50	0.234±0.070	0.207±0.062
		0.6158	2.72	0.155±0.080	0.137±0.070
		0.5763	3.00	0.049±0.023	0.043±0.020
		0.5057	3.50	0.148±0.075	0.131±0.066
p	8	0.7394	1.74	14.9 ±1.5	14.0 ±1.4
		0.6630	2.25	5.34 ±0.85	5.02 ±0.80
		0.6256	2.50	5.30 ±0.63	4.99 ±0.59
		0.5926	2.72	3.69 ±0.62	3.47 ±0.58
		0.5507	3.00	2.41 ±0.33	2.27 ±0.31
		0.4758	3.50	1.64 ±0.27	1.54 ±0.26
π^-	12	0.8891	1.20	21.1 ±1.7	12.2 ±1.0
		0.8614	1.50	12.1 ±1.0	7.02 ±0.56
		0.8152	2.00	1.35 ±0.26	0.78 ±0.15
		0.7783	2.40	0.21 ±0.07	0.12 ±0.04
		0.6767	3.50	<0.06	<0.035
π^+	12	0.8891	1.20	12.8 ±1.9	7.42 ±1.11
		0.8614	1.50	5.95 ±1.1	3.45 ±0.62
		0.8152	2.00	0.88 ±0.41	0.51 ±0.23
		0.7783	2.40	0.52 ±0.21	0.30 ±0.12
p	12	0.8848	1.20	26.5 ±2.4	16.0 ±1.5
		0.8559	1.50	14.3 ±1.4	8.62 ±0.86
		0.8079	2.00	8.81 ±1.2	5.31 ±0.69
		0.7695	2.40	3.64 ±0.91	2.19 ±0.54
		0.7599	2.50	3.30 ±1.1	1.99 ±0.66

dental background subtraction to be made with high statistical accuracy.

E. Hydrogen Target

Liquid hydrogen was contained in a Mylar cylinder of radius 3 in. and length along the beam line of 8.5 in. For several of the runs a 4-in.-long target was also used, which enabled us to check that the solid angle accepted by the counter system was uniform over the length of the target. The walls of the liquid hydrogen vessel were 5- to 15-mil-thick Mylar covered by 20 layers of 0.25-mil-thick aluminized Mylar super-insulation. The vacuum jacket Mylar windows were 10 to 15 mil thick. Elastic scattering runs taken with the target empty always gave a counting rate less than 3% of the full target rate.

F. Backgrounds from Inelastic Processes

Various checks were made to ensure that only elastic scattering events were being detected and not those due to inelastic interactions with two high-momentum charged particles at large angles.

(i) In Geometry 1, proton-proton elastic scattering was simultaneously measured along with the pion-proton scattering by not requiring signals from either of the Čerenkov counters. The results obtained were in good agreement with interpolations between previous measurements. A significant inelastic background would have resulted in p-p cross sections that were too large.

(ii) Runs were taken with liquid nitrogen in the target instead of hydrogen. Typically the counting rate dropped a factor of ~10 when the hydrogen was replaced with nitrogen even though liquid nitrogen is 11.4

TABLE II. Elastic scattering cross sections obtained using Geometry 3.

Incident particle	P_0 (GeV/c)	$\cos\theta_{c.m.}$	$-t$ (GeV/c)^2	u (GeV/c)^2	$(d\sigma/d\omega)_{c.m.}$ (μb/sr)	$d\sigma/dt$[a] (μb/(GeV/c)^2)
π^-	4	−0.9991	6.695	0.084	13.4 ± 4.7	25.2 ± 8.8
		−0.9962	6.686	0.075	16.7 ± 4.7	31.3 ± 8.8
		−0.9848	6.648	0.037	12.2 ± 2.7	22.9 ± 5.1
π^+	4	−0.9962	6.686	0.075	94.3 ±25	177 ±47
		−0.9848	6.648	0.037	53.1 ±12	100 ±23
π^-	8	−1.0000	14.160	0.047	3.78± 1.02	3.35± 0.90
		−0.9991	14.154	0.041	5.63± 1.52	4.99± 1.34
		−0.9962	14.133	0.020	2.41± 0.65	2.13± 0.57
		−0.9914	14.100	−0.013	3.67± 1.00	3.25± 0.88
		−0.9848	14.053	−0.060	3.25± 0.88	2.88± 0.78
π^+	8	−0.9991	14.154	0.041	19.1 ± 6.6	16.9 ± 5.8
		−0.9962	14.133	0.020	13.3 ± 3.1	11.7 ± 2.7
		−0.9914	14.100	−0.013	8.4 ± 2.2	7.4 ± 1.9
		−0.9848	14.053	−0.060	3.2 ± 1.1	2.8 ± 0.9

times more dense. If our detectors had been large enough to accept all quasielastic scattering of pions on the protons in the nitrogen nucleus, the nitrogen counting rate should have been 1.4 times that of the hydrogen rate.[15]

In Geometries 1 and 3 the solid angles and momentum resolutions were so confining that most of the quasielastic scatterings should be lost since the effect of the Fermi momentum of the protons in the nitrogen nucleus would not usually give both of the outgoing particles the correct angle-momentum relationship to be counted by both telescopes. Even if we assume most of our nitrogen rate is due to inelastic rather than quasielastic events, we conclude that Geometries 1 and 3 contain less than 10% inelastic background.

(iii) Some cross sections were measured using both Geometry 1 and Geometry 2. Both geometries gave the same cross sections within errors, whereas inelastic background would cause Geometry 2 to yield larger cross sections due to its larger solid angles.

(iv) Measurements were made of "crossed-channel" events, where a pion telescope was put into coincidence with proton channels other than the one defined by the elastic scattering kinematics, so that only inelastic events could be detected.

These checks indicated that the inelastic background was generally below 5%; hence, a (5±5)% correction to the data was applied. This was true in all cases except the 8 GeV/c points at $-t=4$ and 5 (GeV/c)^2 which were measured only using Geometry 2. The background in this case measured using method (iv) amounted to about 40%, and an additional systematic error of ±20% was added to those results to allow for uncertainties in this subtraction. At $-t=6$ (GeV/c)^2 the background was sufficiently large that only an upper limit to the cross section could be obtained.

G. Corrections and Errors

The measured cross sections were corrected for the muons and electrons in the incident beam (4–8%); absorption in counter telescopes, hydrogen target, and air (10–16%); empty target contribution (3%); the decay of the scattered pions (2% in Geometries 1 and 2, 10% in Geometry 3); and inelastic background dis-

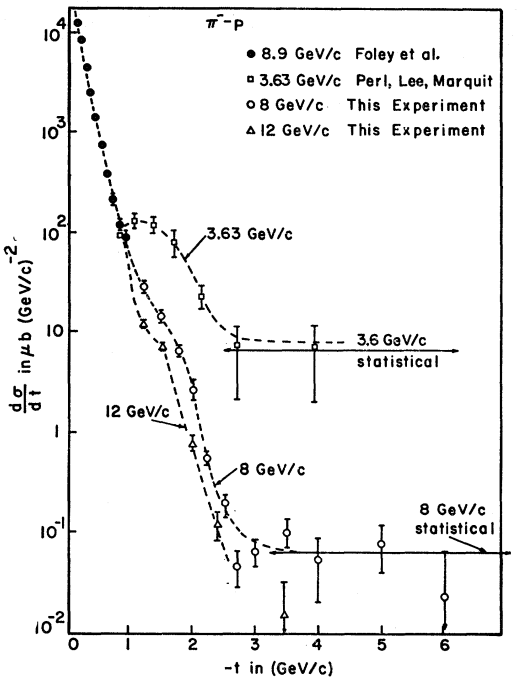

FIG. 6. Angular distributions for π^--p elastic scattering at lab momenta of 3.63, 8, and 12 GeV/c. Curves are drawn only as a guide.

[15] This estimate makes use of the measurement of quasi-elastic scattering cross sections as a function of Z in the paper by G. Bellettini, G. Cocconi, A. N. Diddens, E. Lillethun, G. Matthiae, J. P. Scanlon, and A. M. Wetherell, Nucl. Phys. (to be published).

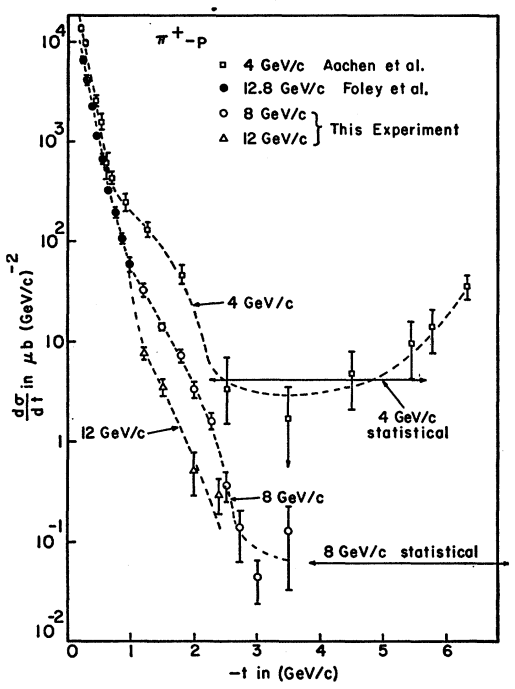

FIG. 7. Angular distributions for π^+-p elastic scattering at lab momenta of 4, 8, and 12 GeV/c. Curves are drawn only as a guide.

cussed in the preceding section. The systematic error due to the uncertainties in the estimation of the above corrections was typically ±10%.

In Geometry 3 there was a large amount of vertical focusing of the scattered pion in the fringe field of the large-aperture magnet. The numerical ray tracings were based on field measurements taken in the median plane and extrapolated values off the median plane using Maxwell's equations. The over-all systematic error in our estimate of vertical angle subtended by the pion counters ranges from 15 to 30% in Geometry 3.

3. DISCUSSION OF RESULTS

The differential cross sections measured in this experiment are listed in Tables I and II. The errors are one standard deviation with statistical and systematic errors added quadratically. The two upper limits listed in the table correspond to 90% confidence intervals. The energy and angular dependence of π^--p scattering is shown in Fig. 6 which for comparison contains the 3.63-GeV/c results of Perl, Lee, and Marquit[16] and the 8.9-GeV/c results of Foley *et al.*[3] Up to $-t\sim1$ (GeV/c)^2, the diffraction peak appears energy-independent. But for larger momentum transfers there is a "shrinkage" with increasing energy. The bump at $-t\sim1.3$ (GeV/c)^2 becomes a shoulder at 8 GeV/c and may still be discerned at 12 GeV/c.

[16] M. L. Perl, Y. Y. Lee, and E. Marquit, Phys. Rev. **138**, B707 (1965).

At higher momentum transfers the cross section continues to drop rapidly until reaching a value consistent with the statistical model of Fast, Hagedorn, and Jones.[17] This reference gives the following formula for the large-angle pion-proton differential cross sections:

$$\frac{d\sigma}{d\omega}\simeq\frac{\sigma_c}{4\pi}\exp[-3.17(s^{1/2}-1.4)], \quad (1)$$

where σ_c is the only free parameter and $s^{1/2}$ is the total energy in the center-of-mass system in GeV. We choose the parameter σ_c to agree with our 8-GeV/c cross section of 0.07 μb/sr and obtain $\sigma_c=3.3$ mb. Then, as shown in Figs. 6 and 7, the predictions for 3.63 and 4 GeV/c agree well with the data. The prediction for 12 GeV/c is a cross section of 5×10^{-3} μb/sr which is almost one order of magnitude lower than the sensitivity of our experiment. The fact that we observed no 12-GeV/c elastic scattering at $-t=3.5$ (GeV/c)^2 is consistent with this prediction of the statistical model. Figure 7 is the same as Fig. 6 except that π^+-p results are plotted rather than π^--p. The general features are the same as for π^--p and there appears to be no strong charge dependence in pion-proton scattering in this energy and angular region.

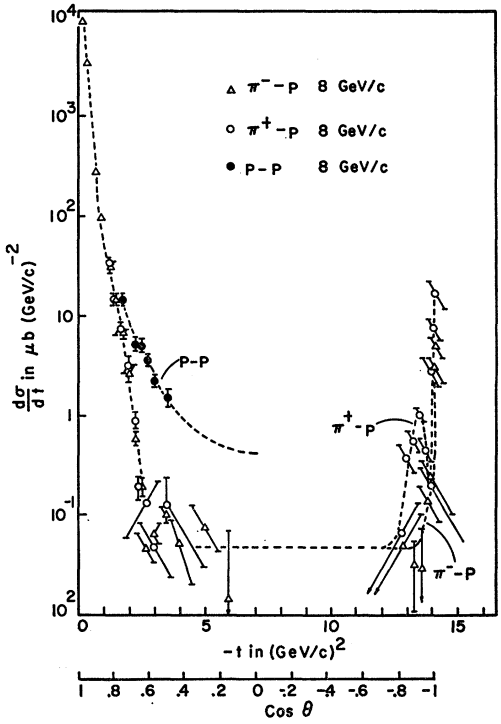

FIG. 8. The complete angular distribution for 8-GeV/c π^+-p and π^--p elastic scattering. p-p elastic scattering cross sections obtained in this experiment at 8 GeV/c are also shown. The large-angle extension of the p-p curve is an interpolation of the results of Refs. 2 and 5. The π-p curves are drawn only as a guide. Data sources same as in Figs. 6, 7, and 9.

[17] G. Fast, R. Hagedorn, and L. W. Jones, Nuovo Cimento **27**, 856 (1963).

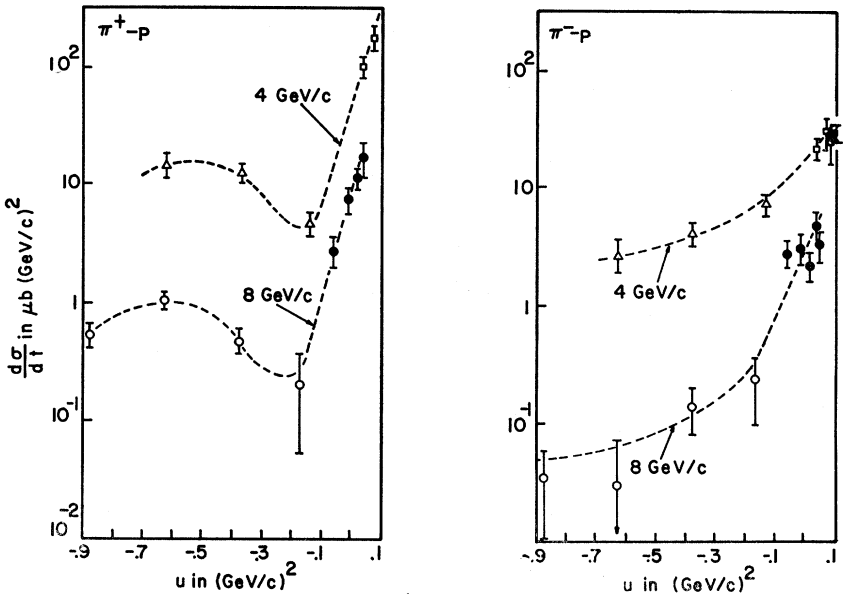

FIG. 9. Pion-proton elastic scattering distributions in the backward peak region at 4 and 8 GeV/c. Results of Ref. 7 are used in addition to the results of this experiment.

■ 4.0 GeV/c Kormanyos *et al.*
△ 4.4 GeV/c } Brody *et al.*
○ 7.8 GeV/c }
□ 4 GeV/c } This exp.
● 8 GeV/c }

The "complete" 8-GeV/c pion-proton angular distribution is shown in Fig. 8 which includes the 150° to 165° data of Brody *et al.*[7] Note that the 150° cross section of Brody *et al.*[7] is about the same as our cross sections in the region of 52° to 73°. Whether or not the cross section in the region $73°<\theta_{c.m.}<150°$ stays close to this same value is not known. No measurements have yet been made in this region. A cross section fairly independent of angle in the region 50° to 150° is favored by the statistical model.[17] Figure 9 is a more detailed view of the 150° to 180° region showing the charge and energy dependences of the backward peaks. Our results plus those of Brody *et al.*[7] are plotted versus u which is the four-momentum transfer squared of the exchange (momentum transfer from initial pion to final proton). For particles of unequal mass u is given by the equation

$$u=\frac{(M^2-\mu^2)^2}{s}-2p^2(1+\cos\theta), \qquad (2)$$

where p is the c.m. momentum, θ is the c.m. scattering angle, and s is the square of the total energy in the c.m. system. We note the existence of a backward peak in all four cases shown in Fig. 9. The data are not accurate enough to determine the precise shapes, but if we assume the same shape as for forward peaks, we can then put limits on the widths of these backward peaks. So for small momentum transfers $[-u<0.2\ (\mathrm{GeV}/c)^2]$ we assume the shape

$$d\sigma/dt \propto e^{Bu} \qquad (3)$$

and fit this function to our cross sections plus the largest angle cross section of Brody *et al.*[7] For π^+-p we obtain the limits $12<B<20\ (\mathrm{GeV}/c)^{-2}$ at 4 GeV/c and $13<B<27\ (\mathrm{GeV}/c)^{-2}$ at 8 GeV/c. For comparison, the pion-proton diffraction peaks in this energy region have the exponent $B=9\ (\mathrm{GeV}/c)^{-2}$. In the case of π^+-p scattering, the backward peaks appear significantly steeper than the forward diffraction peak. For π^--p scattering we obtain the limits $3.8<B<10\ (\mathrm{GeV}/c)^{-2}$ at 4 GeV/c and $10<B<15\ (\mathrm{GeV}/c)^{-2}$ at 8 GeV/c. Only in this last case do the data look almost inconsistent with the shape assumed in Eq. (3). The χ^2 probability for having the six points depart so far from the straight line is about 4%. Perhaps the π^--p backward peak flattens out near 180°. All the cross sections obtained in Geometry 3 are larger than the preliminary values given in Ref. 6. This is because the vertical focusing calculation for the large-aperture magnet is now based on more detailed field measurements. The typical correction amounts to a 30% increase.

There have been several theoretical approaches to explain the backward peak in high-energy pion-proton scattering. One such approach is to consider it as an optical phenomenon.[18,19] Another approach is the coherent droplet model of Byers and Yang.[20] Both these approaches favor similar behavior for π^+-p and π^--p; however, our results show that the backward π^+-p cross section is about five times larger than the π^--p cross section and that the shapes are probably different.

The charge dependence of the backward peak is easier to explain in terms of a baryon exchange model. In π^--p backward scattering, there is double charge exchange and therefore nucleon exchange is forbidden. Since nucleon exchange is permitted in π^+-p elastic scattering, we have a possible explanation for the larger

[18] D. I. Blokhintsev, Nuovo Cimento **23**, 1061 (1962); **31**, 749 (1966).
[19] M. L. Perl, L. W. Jones, and C. C. Ting, Phys. Rev. **132**, 1252 (1963).
[20] N. Byers and C. N. Yang, Phys. Rev. **142**, 976 (1966).

π^+-p backward cross section. In fact the hypothesis of baryon exchange leads to a self-consistent picture if one assumes that the exchange cross section decreases with the mass of the exchanged particle whether it be a boson or a baryon.[21] Simple perturbation theory, however, predicts much larger backward cross sections of broader widths than are observed.[22] Making absorptive and form-factor corrections helps to bring the predictions closer to the experimental results.[23]

It has been suggested by several authors[24–28] that pion-proton backward scattering as opposed to forward scattering might be a cleaner situation for studying the application of Regge-pole formalism to the strong interactions. There are recent papers[29,30] which justify the use of the formula

$$d\sigma_1(u)/d\omega/d\sigma_2(u)/d\omega \simeq \left(\frac{S_1}{S_2}\right)^{2\alpha(u)-1}$$

at $u=0$ when a single Fermion pole dominates. If we make the assumption that only the Δ trajectory [$N^*(1238)$] contributes to π^--p backward scattering, we can use the 4- and 8-GeV/c cross-section values at $u=0$ to obtain $\alpha_\Delta(0)=-0.43\pm0.20$.

If only the Δ trajectory contributed to the π^+-p scattering, the π^+-p backward cross section would be $1/q$ that of the π^--p rather than ~5 times as large. Hence, exchange of $T=\frac{3}{2}$ contributes only about 2% to the π^+-p backward cross section. It is then reasonable to assume that the nucleon trajectory dominates the π^+-p backward scattering. Under this assumption we obtain, using Eq. (3), the result $\alpha_n(0)=-0.42\pm0.13$. At fixed $u=0$ the backward peak energy dependence is then $(d\sigma/d\omega)_{u=0}\propto S^{-1.8\pm0.3}$. At fixed angle of 180°, which is not the same as a fixed u, the energy dependence would be $(d\sigma/d\omega)_{180°}\propto S^{-2.1\pm0.3}$.[31] Even though most theories of the backward peak predict a drop with energy by a power law rather than the more rapid drop of an exponential, our measurements being at lonly two energies cannot settle this question. Measurements at higher energies are needed.

In summary, the 4-, 8-, and 12-GeV/c pion-proton angular distributions, although orders of magnitude different in large-angle scattering, possess certain similarities. At low momentum transfer the forward diffraction peaks are all the same and all have structure at $-t\sim1.3$ (GeV/c)^2 followed by a fast drop in cross section until a value compatible with the statistical-model formula [Eq. (1)] is reached. Then the angular distributions might be reasonably flat until the backward peak is reached. The backward peaks drop more slowly with energy than the "flat" 90° regions. More experiments are needed to see if higher energy pions will follow the same pattern.

ACKNOWLEDGMENTS

We wish to thank Dr. W. Baker for his contributions to the planning and early stages of this experiment. We are indebted to the staff of the Brookhaven AGS for their assistance and cooperation. In particular we are grateful to Dr. R. Cool for valuable advice and to O. Thomas, H. Sauter, and G. Munoz of the Cool group for their assistance. We thank E. Coleman for help during part of the run.

[21] So far, in all cases of observed forward and backward peaks the exchanged quantum numbers can be identified with existing bosons or baryons; and where the exchange would involve a doubly charged boson or a baryon of positive strangeness the corresponding peaks are notably absent. So far, all forward and backward peaks seem to drop with energy at the same rate. Whether or not strangeness is exchanged, a crude rule of thumb is that the relative cross sections vary inversely as the square of the mass of the exchanged particle.

[22] V. Cook, B. Cork, W. R. Holley, and M. L. Perl, Phys. Rev. **130**, 762 (1963).

[23] R. M. Heinz and M. H. Ross, Phys. Rev. Letters **14**, 1091 (1965).

[24] D. C. Frautschi, M. Gell-Mann, and F. Zachariasen, Phys. Rev. **126**, 2204 (1962).

[25] V. N. Gribov, Zh. Eksperim. i Teor. Fiz. **43**, 1529 (1962) [English transl.: Soviet Phys.—JETP **16**, 1080 (1963)].

[26] G. F. Chew and J. D. Stack, University of California Radiation Laboratory Report No. UCRL-16293 (unpublished).

[27] J. D. Stack, Phys. Rev. Letters **16**, 286 (1966).

[28] V. Barger and D. Cline, Phys. Rev. Letters **16**, 916 (1966).

[29] D. Z. Freedman and J. M. Wang, Phys. Rev. Letters **17**, 569 (1966).

[30] M. L. Goldberger and C. E. Jones, Phys. Rev. **150**, 1269 (1966).

[31] This energy dependence is consistent with the energy dependence of the 180° π^--p cross section using the data above 2.5 GeV/c reported in Ref. 12 and averaging out structure due to possible resonances.